



UNIVERSITY OF LEEDS

This is a repository copy of *Bimolecular Reactions of Activated Species: An Analysis of Problematic HC(O)C(O) chemistry*.

White Rose Research Online URL for this paper:  
<http://eprints.whiterose.ac.uk/104220/>

Version: Supplemental Material

---

**Article:**

Shannon, RJ, Robertson, SH, Blitz, MA et al. (1 more author) (2016) Bimolecular Reactions of Activated Species: An Analysis of Problematic HC(O)C(O) chemistry. *Chemical Physics Letters*, 661. pp. 58-64. ISSN 0009-2614

<https://doi.org/10.1016/j.cplett.2016.08.055>

---

© 2016 Elsevier B.V. Licensed under the Creative Commons Attribution-NonCommercial-NoDerivatives 4.0 International  
<http://creativecommons.org/licenses/by-nc-nd/4.0/>

**Reuse**

Unless indicated otherwise, fulltext items are protected by copyright with all rights reserved. The copyright exception in section 29 of the Copyright, Designs and Patents Act 1988 allows the making of a single copy solely for the purpose of non-commercial research or private study within the limits of fair dealing. The publisher or other rights-holder may allow further reproduction and re-use of this version - refer to the White Rose Research Online record for this item. Where records identify the publisher as the copyright holder, users can verify any specific terms of use on the publisher's website.

**Takedown**

If you consider content in White Rose Research Online to be in breach of UK law, please notify us by emailing [eprints@whiterose.ac.uk](mailto:eprints@whiterose.ac.uk) including the URL of the record and the reason for the withdrawal request.



[eprints@whiterose.ac.uk](mailto:eprints@whiterose.ac.uk)  
<https://eprints.whiterose.ac.uk/>

# Observation of a New Channel, the Production of CH<sub>3</sub>, in the Abstraction Reaction of OH Radicals with Acetaldehyde

Neil U. M. Howes, James P. A. Lockhart<sup>†</sup>, Mark A. Blitz<sup>1\*</sup>, Scott A. Carr, Maria Teresa Baeza-Romero<sup>+</sup>, Dwayne E. Heard<sup>1</sup>, Robin J. Shannon<sup>‡</sup>, Paul W. Seakins<sup>1\*</sup> and T. Varga<sup>#</sup>

School of Chemistry, University of Leeds, Leeds, LS2 9JT, UK.

<sup>1</sup> National Centre for Atmospheric Science, University of Leeds, Leeds, LS2 9JT, UK.

## Supplementary Information

### Contents

- 1.0 Experimental Details
- 2.0 Calibration Method
- 3.0 Mechanism for fitting OH/CH<sub>3</sub>CHO/O<sub>2</sub> experiments (Fig 3 of main manuscript)
- 4.0 Investigation of possible interferences from secondary chemistry
- 5.0 Details on Pressure Dependence of the Methyl Yield from Reaction 1
- 6.0 References

### 1.0 Experimental Details

#### 1.1 Laser Flash Photolysis/Photoionization Mass Spectrometry (LFP/PIMS) System

Figure S1 shows a schematic of the apparatus and Figure S2 further details of the flow-tube, sampling and TOFMS system.

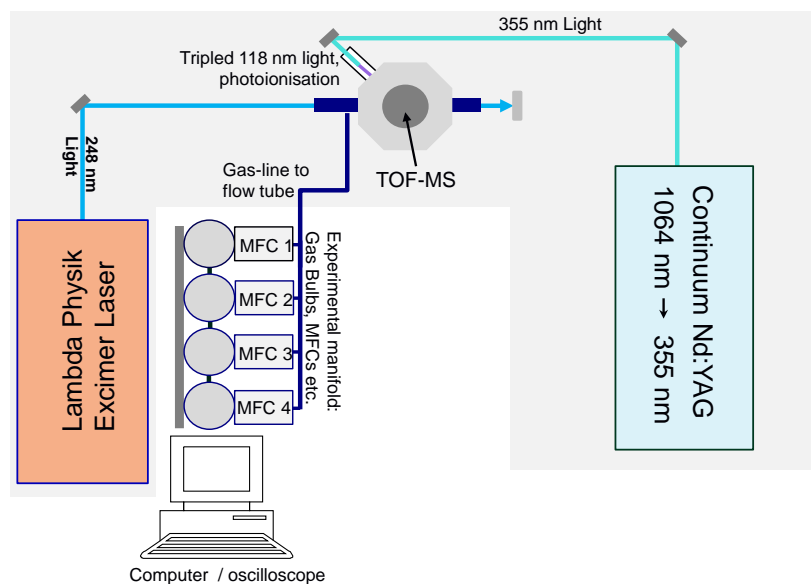


**Figure S1.** Schematic of the PIMS system.

The photolysis laser is a Lambda Physik Compex 205 operated at 10 Hz. The typical gas residence time was  $< 0.05$  s, ensuring the photolysis of a fresh gas mix for each laser pulse. Typical energy densities were  $10 - 50 \text{ mJ cm}^{-2}$ .

OH radicals were generated via a variety of methods as detailed in the main manuscript. For the kinetic studies, the photolysis of oxalyl chloride,  $(\text{COCl})_2$ , was used to produce Cl atoms.<sup>1</sup> As detailed in section 2.0 the photolysis of acetylchloride was another Cl source used in the calibration process.

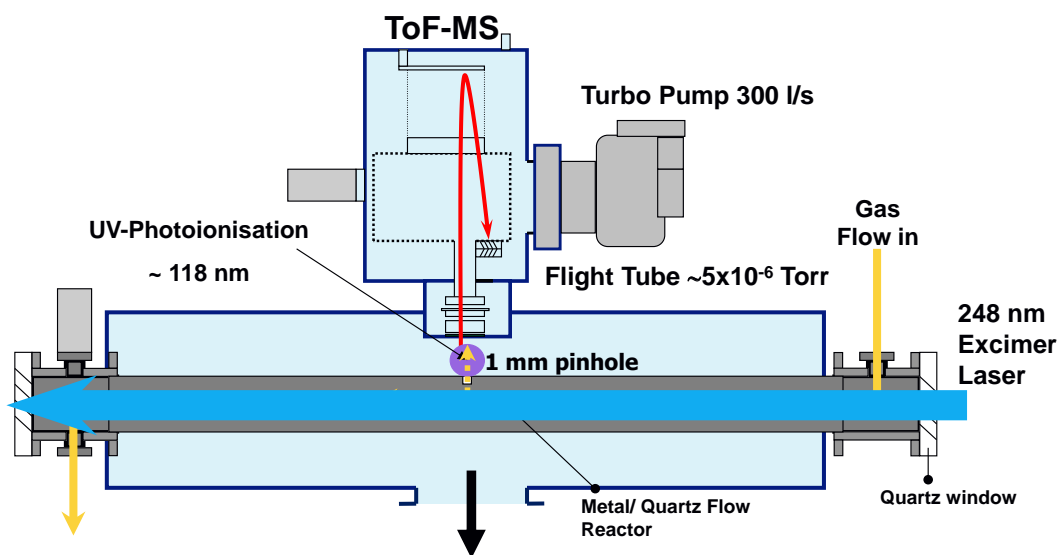


**Figure S2.** Details of the flow system, sampling and TOFMS.

The VUV radiation for photoionization was generated by frequency tripling the 355 nm output of a YAG laser (Continuum, Powerlite 8010) in xenon (total pressure ~ 50 Torr in a glass cell). The frequency tripling gas cell was coupled directly to the ionization chamber with a MgF<sub>2</sub> window. Ions generated by the VUV laser pulse were focused into a reflectron time of flight mass spectrometer (TOFMS, Kore Instruments) and were detected via dynode detectors (ETP Electron Multipliers, AF824).

If the rate coefficient for the chemical reaction is  $< 500 \text{ s}^{-1}$  then the time taken for sampling can be ignored and this is the approach that has been used in previous systems, for example those of Gutman and Slagle.<sup>2</sup> However, in a previous publication<sup>3</sup> we have shown that the transit time to the low pressure ionization region can be accounted for, extending the maximum pseudo-first-order rate coefficient which can reliably be extracted from this apparatus to  $>10,000 \text{ s}^{-1}$ . Equation E1 in the main manuscript provides a completely general expression for the radical signal, but it can be significantly simplified if there is no initial radical production or if the chemical rate coefficient is  $< 500 \text{ s}^{-1}$ .

## 1.2 Laser Flash Photolysis/Laser Induced Fluorescence (LFP/LIF) System

Figure S3 shows a schematic of the LFP/LIF system. Details on the photolysis system and OH radical generation are given in the main manuscript.

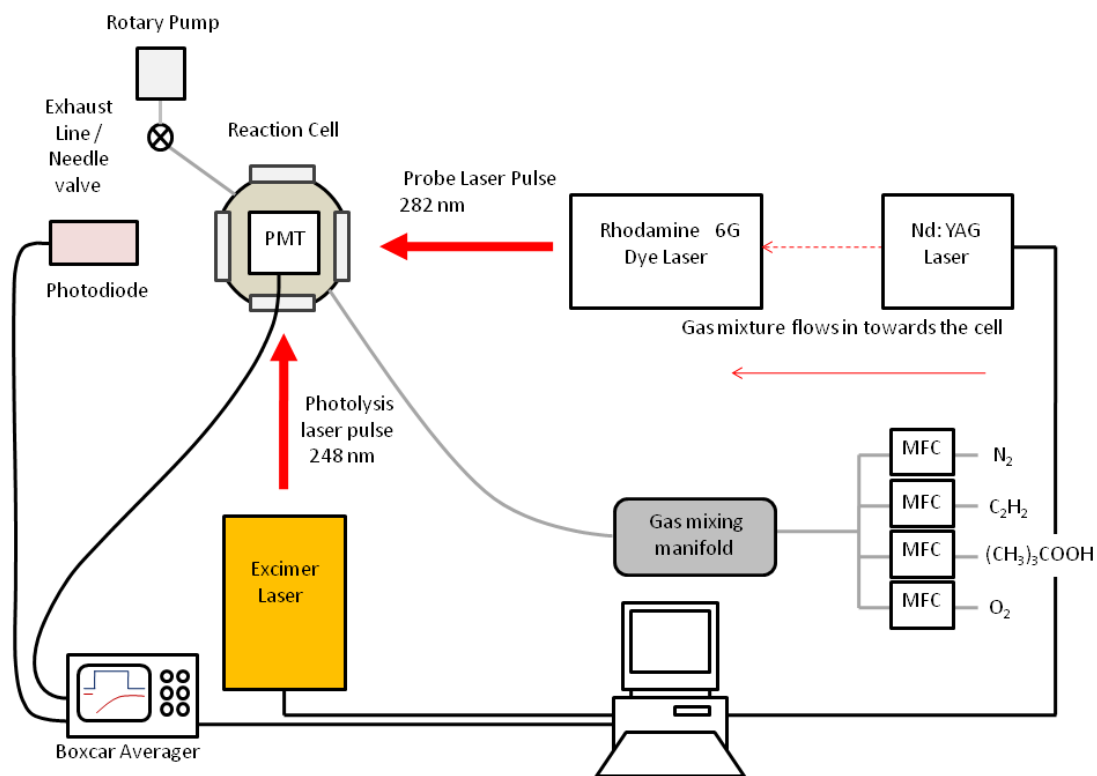


**Figure S3.** Schematic of the LFP/LIF system.

OH radicals were detected by off-resonance LIF with excitation taking place at  $\sim 282$  nm ( $A^2\Sigma(v=1) \leftarrow X^2\Pi(v=0)$ ,  $Q_1(1)$ ) with the fluorescence being observed at  $\sim 308$  nm through an interference filter (Corion,  $310 \pm 10$  nm) by a photomultiplier tube mounted perpendicular to the plane of the probe and photolysis lasers. Probe radiation was generated from a YAG (Spectra Physik GCR-150) pumped dye laser (Spectra Physik PDL-3 Rhodamine6G) for OH observation. The photomultiplier signal was integrated using a boxcar average (SRS) and digitized before being sent to a personal computer for data analysis. The time delay between the photolysis and probe lasers was varied to build up a record of the OH signal following photolysis. Kinetic traces typically contained 200 – 400 data points, each of which was averaged 2 - 10 times depending on the signal-to-noise ratio.

## 2.0 CH<sub>3</sub> and CH<sub>3</sub>CO Calibration

### 2.1 Calibration Method for 248 nm Photolysis

Figure S4 shows schematically the production of CH<sub>3</sub> and CH<sub>3</sub>CO radicals from Reaction 1.



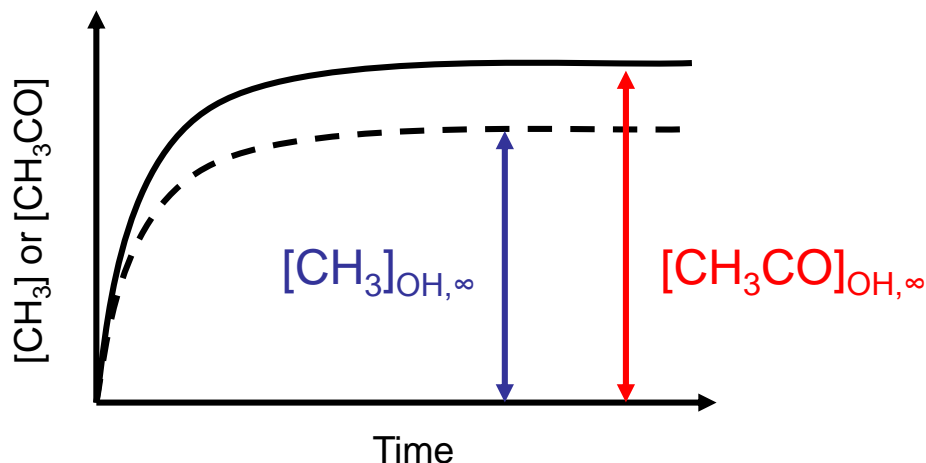


**Figure S4.** Schematic defining the terms for the branching ratio to methyl radicals from reaction 1.

In order to calculate the branching ratio to methyl,  $Y_{\text{CH}_3}$ :

$$Y_{\text{CH}_3} = \frac{[\text{CH}_3]_{\text{OH},\infty}}{[\text{CH}_3\text{CO}]_{\text{OH},\infty} + [\text{CH}_3]_{\text{OH},\infty}} = 1 + \frac{[\text{CH}_3]_{\text{OH},\infty}}{[\text{CH}_3\text{CO}]_{\text{OH},\infty}}$$

the ratio  $[\text{CH}_3]:[\text{CH}_3\text{CO}]$  needs to be determined. As mentioned in the main manuscript, determining this ratio is complicated by the fact that  $\text{CH}_3^+$  ions are formed from  $\text{CH}_3\text{CO}$  and therefore:

$$(S_{\text{CH}_3})_{\text{OH},\infty} = \alpha[\text{CH}_3]_{\text{OH},\infty} + \beta[\text{CH}_3\text{CO}]_{\text{OH},\infty}$$

$$(S_{\text{CH}_3\text{CO}})_{\text{OH},\infty} = \gamma[\text{CH}_3\text{CO}]_{\text{OH},\infty}$$

where  $(S_x)_{\text{OH},\infty}$  is the long-time signal of  $\text{CH}_3$  or  $\text{CH}_3\text{CO}$  and  $\alpha$ ,  $\beta$ ,  $\gamma$  link the ion signal to the concentration.

The experimentally determined ratio of the long-time signals is therefore given by:

$$\frac{(S_{\text{CH}_3})_{\text{OH},\infty}}{(S_{\text{CH}_3\text{CO}})_{\text{OH},\infty}} = \frac{\alpha[\text{CH}_3]_{\text{OH},\infty} + \beta[\text{CH}_3\text{CO}]_{\text{OH},\infty}}{\gamma[\text{CH}_3\text{CO}]_{\text{OH},\infty}}$$

$$\frac{(S_{\text{CH}_3})_{\text{OH},\infty}}{(S_{\text{CH}_3\text{CO}})_{\text{OH},\infty}} = \frac{\alpha}{\gamma} \frac{[\text{CH}_3]_{\text{OH},\infty}}{[\text{CH}_3\text{CO}]_{\text{OH},\infty}} + \frac{\beta}{\gamma}$$

Calibration therefore requires the determination of  $\alpha/\gamma$  and  $\beta/\gamma$ .

Reaction 9 provides a good method of determining  $\beta/\gamma$ .



The lower exothermicity of reaction 9 compared to reaction 1 prevents acetyl fragmentation and therefore any methyl signal must arise from fragmentation in the ionization process.

$$\begin{aligned} (S_{\text{CH}_3})_{\text{Cl},\infty} &= \beta[\text{CH}_3\text{CO}]_{\text{Cl},\infty} \\ (S_{\text{CH}_3\text{CO}})_{\text{Cl},\infty} &= \gamma[\text{CH}_3\text{CO}]_{\text{Cl},\infty} \\ \frac{(S_{\text{CH}_3})_{\text{Cl},\infty}}{(S_{\text{CH}_3\text{CO}})_{\text{Cl},\infty}} &= \frac{\beta}{\gamma} \end{aligned}$$

Photolysis of acetyl chloride in the presence of excess acetaldehyde, where the yield of  $\text{CH}_3:\text{CH}_3\text{CO}$  is known (0.55:0.45) allows for the determination of  $\alpha/\gamma$ . Figure S5 shows a schematic of the acetyl chloride photolysis.  $\text{CH}_3$  and  $\text{CH}_3\text{CO}$  are produced in the initial photolysis and  $[\text{Cl}]_0 = [\text{CH}_3]_0 + [\text{CH}_3\text{CO}]_0$ . The Cl atoms subsequently react with acetaldehyde producing acetyl only (reaction 9). Any long-time methyl signal therefore arises from fragmentation in the ionization process.

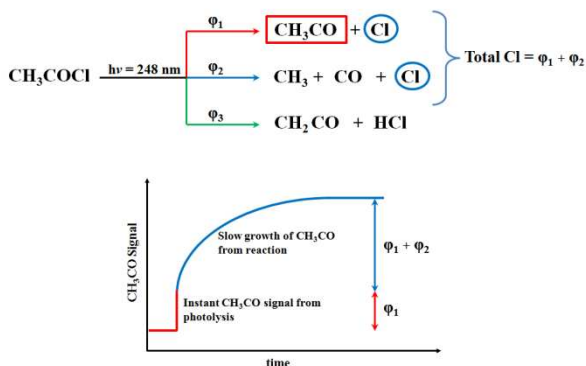


**Figure S5a.** Schematic of contributions to the signal

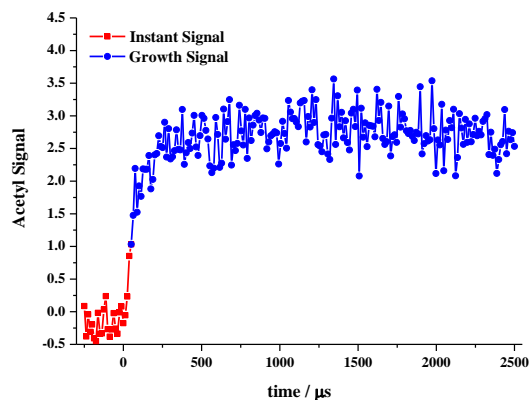


**Figure S5b:** Example of  $\text{CH}_3\text{CO}$  signal

$$\begin{aligned}
(S_{\text{CH}_3})_{\text{AcCl},0} &= \alpha[\text{CH}_3]_{\text{AcCl},0} + \beta[\text{CH}_3\text{CO}]_{\text{AcCl},0} \\
[\text{CH}_3] &= 1.25[\text{CH}_3\text{CO}] \\
(S_{\text{CH}_3})_{\text{AcCl},0} &= \alpha 1.25[\text{CH}_3\text{CO}]_{\text{AcCl},0} + \beta[\text{CH}_3\text{CO}]_{\text{AcCl},0} \\
(S_{\text{CH}_3\text{CO}})_{\text{AcCl},0} &= \gamma[\text{CH}_3\text{CO}]_{\text{AcCl},0} \\
\frac{(S_{\text{CH}_3})_{\text{AcCl},0}}{(S_{\text{CH}_3\text{CO}})_{\text{AcCl},0}} &= \frac{\alpha 1.25[\text{CH}_3\text{CO}]_{\text{AcCl},0} + \beta[\text{CH}_3\text{CO}]_{\text{AcCl},0}}{\gamma[\text{CH}_3\text{CO}]_{\text{AcCl},0}} \\
\frac{(S_{\text{CH}_3})_{\text{AcCl},0}}{(S_{\text{CH}_3\text{CO}})_{\text{AcCl},0}} &= 1.25 \frac{\alpha}{\gamma} + \frac{\beta}{\gamma}
\end{aligned}$$

$\beta/\gamma$  is known from the above study and hence  $\alpha/\gamma$  can be calculated.

## 2.2 Calibration Method for 193 nm Photolysis

The methyl radical data collected from the acetone photolysis experiments were calibrated to mimic the  $\text{N}_2\text{O}$  environment used in the ethanal + OH reactions. The photolytic acetone signal was tuned to  $[\text{N}_2\text{O}]$  so that the  $\text{CH}_3$  signal observed could be equated to the  $\text{CH}_3$  signal measured in the ethanal + OH experiments.

$$M_{\text{A1}} = M_{\text{A0}} \times \frac{[\text{N}_2\text{O}] \cdot \sigma_{\text{N}_2\text{O}} \cdot n_c}{[\text{CH}_3\text{COCH}_3] \cdot \sigma_{\text{CH}_3\text{COCH}_3}} \quad (\text{ES1})$$

Here  $M_{\text{A1}}$  is the adjusted methyl signal from photolytic acetone,  $M_{\text{A0}}$  is the raw methyl radical signal from acetone experiments and  $\sigma$  represent the relevant cross-sections of the two species ( $\text{N}_2\text{O}$  and acetone respectively). Finally  $n_c$  is a factor used to balance the equation based on the conversion of  $\text{N}_2\text{O}$  to OH, this was estimated from the NO signal monitored during the experiments (NO is produced from  $\text{O}(^1\text{D}) + \text{N}_2\text{O}$ ).

The adjusted methyl signal from acetone photolysis was then compared with methyl signal obtained from the ethanal + OH experiments. This parameter,  $f_{\frac{M_{\text{OH}}}{M_{\text{A1}}}}$ , can be thought of as the

fraction of  $\text{CH}_3$  formed from the reaction with OH in comparison to the maximum  $\text{CH}_3$  signal. This component was then multiplied by the parameter analogous to the proportional difference in  $\text{CH}_3:\text{CH}_3\text{CO}$  signal ratios obtained from OH and Cl experiments,  $f_{\frac{S_{\text{ROH}} - S_{\text{RCl}}}{S_{\text{ROH}}}}$ . This calculation gives

evaluation of the yield of methyl radicals:

$$Y_{\text{CH}_3} (\%) = f_{\frac{M_{\text{OH}}}{M_{\text{A1}}}} \times f_{\frac{S_{\text{ROH}} - S_{\text{RCl}}}{S_{\text{ROH}}}} \times 100 \quad (\text{ES2})$$

### 3.0 Mechanism used to fit CH<sub>3</sub>/CH<sub>3</sub>CO/lactone signal in Fig 3

The following mechanism was used to simulate the temporal profiles of CH<sub>3</sub>, CH<sub>3</sub>CO and the signal at  $m/z = 42$  (associated with lactone production) that were obtained in the presence of small amounts of oxygen. The rate coefficients for the first order removal of CH<sub>3</sub>, CH<sub>3</sub>CO (diffusion and wall loss) were obtained from the decays of CH<sub>3</sub> and CH<sub>3</sub>CO at long times in the absence of oxygen and were used as estimates for OH and lactone loss. The pseudo-first-order rate coefficient for OH reaction with acetaldehyde, typically  $1 \times 10^{14}$  molecule cm<sup>-3</sup>, is very large compared to wall loss ( $>1500$  s<sup>-1</sup>:100 s<sup>-1</sup>), so the effect of uncertainties in the OH wall/diffusion loss will be small. The wall loss of the stable lactone is likely to be lower than that for CH<sub>3</sub> or CH<sub>3</sub>CO, but does not substantially effect the quality of the fit.

**Table S1** Mechanism for Fitting data in Figure 3

Reaction	Rate coefficient/ cm <sup>3</sup> molecule <sup>-1</sup> s <sup>-1</sup>	Reference
OH + CH <sub>3</sub> CHO → H <sub>2</sub> O + CH <sub>3</sub> CO	$0.85 \times 1.5 \times 10^{-11}$	IUPAC <sup>a</sup>
OH + CH <sub>3</sub> CHO → H <sub>2</sub> O + CH <sub>3</sub> + CO	$0.15 \times 1.5 \times 10^{-11}$	IUPAC <sup>a</sup>
CH <sub>3</sub> + O <sub>2</sub> + M → CH <sub>3</sub> O <sub>2</sub> + M	$5 \times 10^{-14}$	IUPAC <sup>b</sup>
CH <sub>3</sub> CO + O <sub>2</sub> → lactone + OH	$2 \times 10^{-12}$	Carr et al. <sup>4</sup>
CH <sub>3</sub> CO →	fitted	
CH <sub>3</sub> →	fitted	

a IUPAC<sup>5</sup> with branching ratio scaled to this work. The possible minor channel to CH<sub>2</sub>CHO + H<sub>2</sub>O has been ignored.

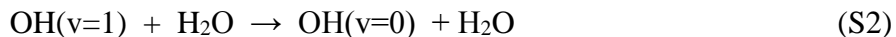
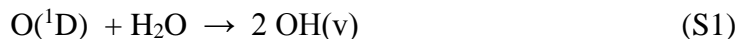
b The IUPAC evaluation which has been used is for N<sub>2</sub> as a bath gas and is therefore likely to be a slight overestimate for this work in He, however, CH<sub>3</sub> loss via this reaction is negligible.

### 4.0 Investigation into possible secondary chemistry

The experiments at 193 nm produced a consistent yield, even when the electron multiplier used to detect the radicals was changed; this consistency suggests that the methodology used was reliable. However, initially there was some concern with these experiments, particularly with the monitored NO signal.

When water was bubbled into the system the monitored NO signal did not completely subside, this means that not all of the O(<sup>1</sup>D) reacted with water to OH. The best explanation for this is that the concentration of water was lower than was expected. Using the NO signal data the water concentration was extrapolated and evaluated at approximately  $8 \times 10^{14}$  cm<sup>-3</sup>. This is significantly lower than the concentration previously determined, which suggested  $[\text{H}_2\text{O}] \approx 2 \times 10^{15}$  cm<sup>-3</sup>. This result suggests a sizable portion of the water was lost to the walls.

In addition to removing O(<sup>1</sup>D) from the reaction system, water is also plays an important role in quenching vibrationally excited hydroxyl radicals, OH(v).



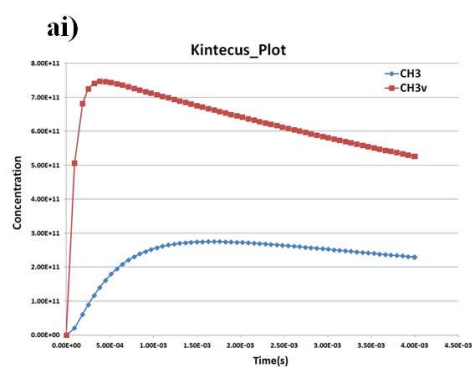
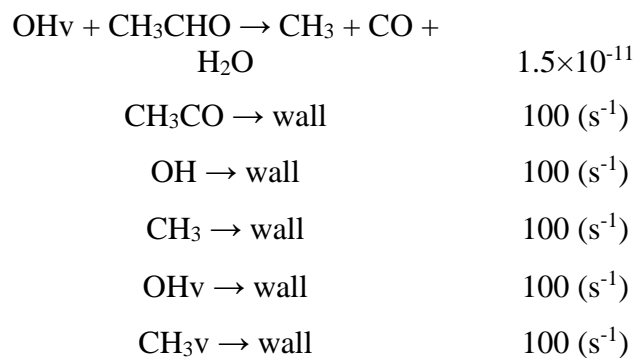
If there is a significant proportion of the OH(v) radicals formed are left unquenched it could majorly interfere with the observed methyl radical yield. For example, in the reaction between OH(v=1) and CH<sub>3</sub>CHO it is assumed to yield 1 CH<sub>3</sub> methyl for every OH(v=1) radical reacted:



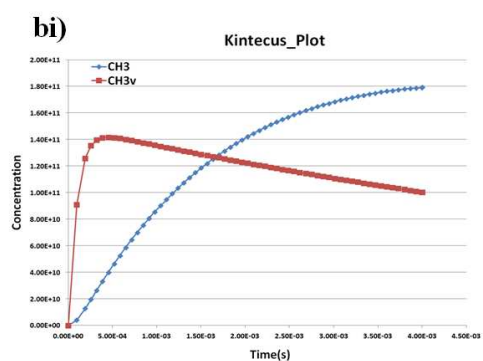
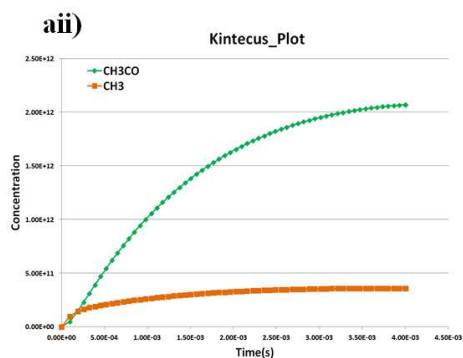
If this were the case it would lead amplification in the methyl radical yield making the above results invalid. To test the validity of these experiments a Kintecus<sup>6</sup> model was run, the reaction scheme and the initial conditions are listed in Table S2. In this reaction system under these experimental conditions much depends on the rate of OH(v=1) quenching by H<sub>2</sub>O, k<sub>q</sub>. However, there appears to be a considerable discrepancy between the literature values. Most early work seems to suggest a quenching rate constant between 2.5 -7.5 × 10<sup>-10</sup> cm<sup>3</sup> s<sup>-1</sup> <sup>7</sup>, but more recent work indicates a lower rate of k<sub>q</sub> ≈ 1 × 10<sup>-11</sup> cm<sup>3</sup> s<sup>-1</sup> <sup>8</sup>. Clearly, if the quenching rate coefficient is smaller then there will be more OH(v=1) present in the system and therefore reaction S3 will have greater importance. In the model a lower limit of k<sub>q</sub> was used to maximise the influence of this channel.

**Table S2.** a) Kintecus model + rate coefficients, k. Units of k are cm<sup>3</sup>s<sup>-1</sup> unless otherwise stated. b) Shows the initial conditions assumed. T= 298 K for all modelling.

a)	k	b)	
Reaction in the kintecus model		Reactants	Concentrations
O( <sup>1</sup> D) + N <sub>2</sub> O → NO + NO	1.5×10 <sup>-10</sup>	O( <sup>1</sup> D)	5. ×10 <sup>12</sup>
O( <sup>1</sup> D) + H <sub>2</sub> O → OHv + OHv	2.0×10 <sup>-10</sup>	N <sub>2</sub> O	1.×10 <sup>15</sup>
OHv +H <sub>2</sub> O → OH + H <sub>2</sub> O	1.25×10 <sup>-11</sup>	H <sub>2</sub> O	8 ×10 <sup>14</sup>
OH + CH <sub>3</sub> CHO → CH <sub>3</sub> CO + H <sub>2</sub> O	1.5×10 <sup>-11</sup>	CH <sub>3</sub> CHO	2 - 10 ×10 <sup>13</sup>
OH + CH <sub>3</sub> CHO → CH <sub>3</sub> + CO + H <sub>2</sub> O	1.5×10 <sup>-12</sup>		



[acetaldehyde] =  $2 \times 10^{13} \text{ cm}^{-3}$



[acetaldehyde] =  $1.2 \times 10^{14} \text{ cm}^{-3}$

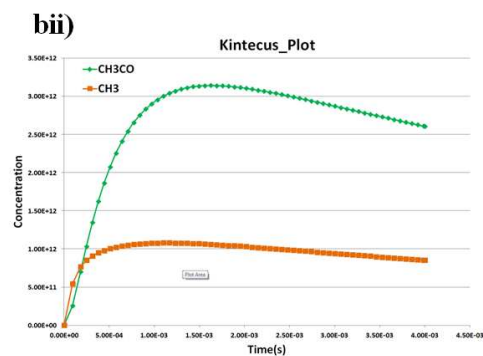


**Figure S6.** graphs ai) and bi) the concentrations of  $\text{CH}_3$  radical formed from ethanal +  $\text{OH}(v=1)$ (red) and ethanal +  $\text{OH}$  (blue) are shown. In graph aii) and bii) the relationship between the concentrations of  $\text{CH}_3$  radicals (orange) and  $\text{CH}_3\text{CO}$  radicals (green) for varying ethanal concentrations is shown.

Figure S6 shows two sets of graphs with varying initial concentrations of acetaldehyde used: for graphs a)  $[\text{acetaldehyde}] = 2 \times 10^{13} \text{ cm}^{-3}$  and in graphs b)  $[\text{acetaldehyde}] = 1.2 \times 10^{14} \text{ cm}^{-3}$ . In graphs ai) and bi) the concentrations of  $\text{CH}_3$  radical formed from ethanal +  $\text{OH}(v=1)$ (red) and ethanal +  $\text{OH}$  (blue) are shown. Both plot show a significant  $\text{CH}_3$  radical component from the

OH( $v=1$ ) channel, unsurprisingly this effect is greater at larger acetaldehyde concentrations. If indeed modelled behaviour is real it indicates that a large fraction of the  $Y_{\text{CH}_3}$  measured is actually due to the reaction between ethanal + OH( $v=1$ ) and not because of the chemically activated fragmentation of acetyl radicals. In graph aii) and bii) the relationship between the concentrations of  $\text{CH}_3$  radicals (orange) and  $\text{CH}_3\text{CO}$  radicals (green) is shown for different acetaldehyde concentrations. From these graphs it is shown that the model predicts larger methyl radical yields at higher acetaldehyde concentration. Crucially, this was not observed experimentally (see Figure S7).

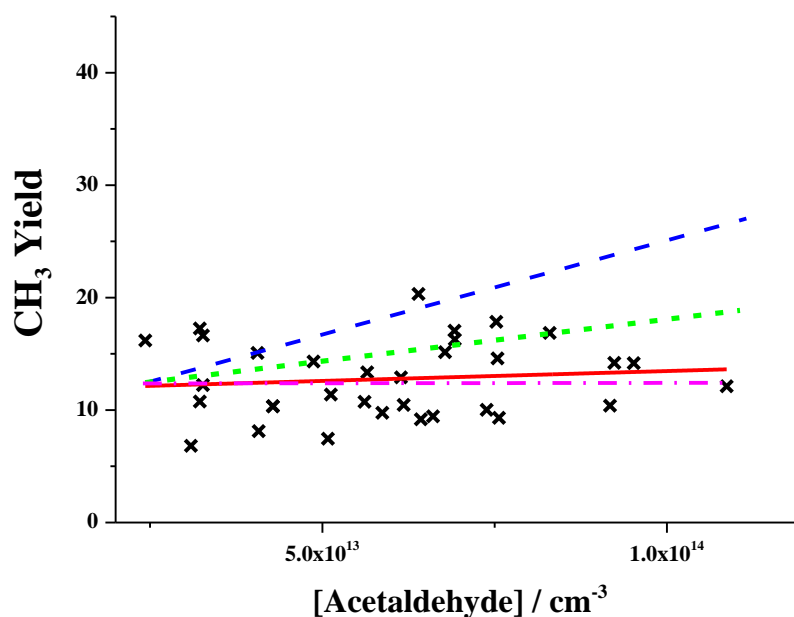


**Figure S7.** A plot showing the measured and modelled the dependency of the  $\text{CH}_3$  yield on [acetaldehyde]

In Figure S7 the  $\text{CH}_3$  yields measured experimentally are plotted against the concentration of acetaldehyde. Theoretically the yield of methyl radicals formed should not vary with concentration if the source of the methyl radicals is from chemically activated decomposition of acetyl radicals (pink line). Figure S7 indicates there is a small dependency on acetaldehyde concentration (red line), with slightly larger  $\text{CH}_3$  yield predicted at higher ethanal concentrations ( $Y_{\text{CH}_3} = 12.4\%$  at  $[\text{CH}_3\text{CHO}] = 2.5 \times 10^{13} \text{ cm}^{-3}$  and  $Y_{\text{CH}_3} = 13.5\%$  at  $[\text{CH}_3\text{CHO}] = 1 \times 10^{14} \text{ cm}^{-3}$ ). However, if a significant fraction of the methyl radical yield was caused by the reaction between acetaldehyde + OH( $v=1$ ) reaction then the increase in  $Y_{\text{CH}_3}$  at high acetaldehyde concentrations would be much greater than was observed experimentally (Figure S7, blue line) ( $Y_{\text{CH}_3} = 12.8\%$  at  $[\text{CH}_3\text{CHO}] = 2.5 \times 10^{13} \text{ cm}^{-3}$  and  $Y_{\text{CH}_3} = 25.4\%$  at  $[\text{CH}_3\text{CHO}] = 1 \times 10^{14} \text{ cm}^{-3}$ ).

There are two possible reasons for the discrepancy between the experimental and modelled data. It may be because the NO data measured do not give an accurate evaluation of the water concentration. However, multiple experiments were conducted over several days and were fairly consistent ( $\pm 10\%$ ). A second and possibly more likely explanation is the rate of OH(v=1) quenching by H<sub>2</sub>O is larger than was used for modelling. If a quenching rate coefficient of  $k_q = 1 \times 10^{-10} \text{ cm}^3\text{s}^{-1}$  is used in the model then the  $Y_{\text{CH}_3}$  is nearly independent of acetaldehyde concentration. In Figure S8 it can be seen in plots ai) and bi) that there is still a small contribution to the  $Y_{\text{CH}_3}$  from the ethanal + OH(v=1) channel ( $5\% < \text{RS3} < 15\%$ ).

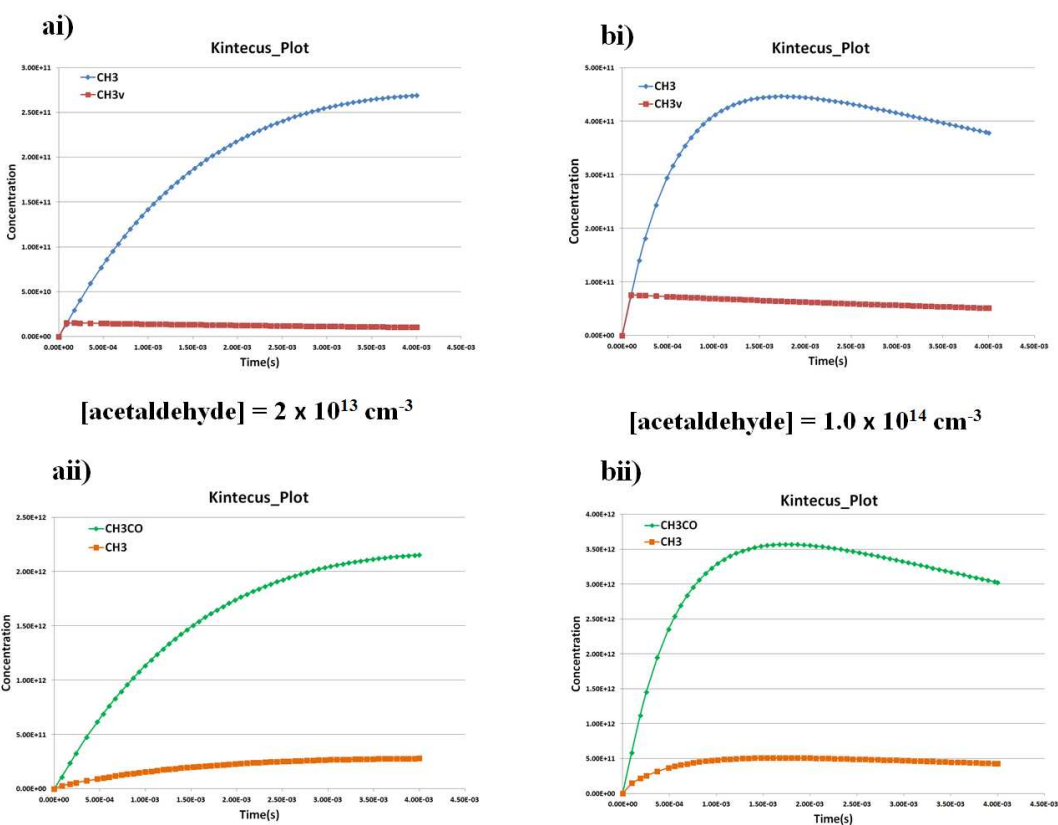


**Figure S8.** Graphs ai) and bi) the concentrations of CH<sub>3</sub> radical formed from ethanal + OH(v=1)(red) and ethanal + OH (blue) are shown. In graph aii) and bii) the relationship between the concentrations of CH<sub>3</sub> radicals (orange) and CH<sub>3</sub>CO radicals (green) for varying ethanal concentrations is shown.

Note: the reaction between O(<sup>1</sup>D) + CH<sub>3</sub>CHO was also modelled (green line, Figure S7), like the OH(v) channel this reaction suggests a dependency on acetaldehyde concentration. As there was only a slight dependency on [acetaldehyde] observed this too suggests that the dominant process for methyl radical formation is R1e.

However, this does mean that the CH<sub>3</sub> radical yields predicted from these experiments may slightly over predict the chemically activated acetyl fragmentation channel. The analysis was redone to

take the minor OH( $v=1$ ) and O( $^1D$ ) contributions into account. A concentration dependent parameter was used to adjust the methyl yields. This analysis lowered the methyl radical yield for the chemically activated acetyl fragmentation by approximately 20 %, giving a new  $Y_{CH_3} = (13.6 \pm 4.0) \%$ .

### 5.0 Details on Pressure Dependence of the Methyl Yield from Reaction 1

Figure S9 shows the calculated yields as a function of total pressure for three different bath gases, He, N<sub>2</sub> and air and for each bath gas a representative range of values for  $\langle \Delta E_{down} \rangle$  (100-200  $cm^{-1}$  for He and 250-350  $cm^{-1}$  for N<sub>2</sub> and air)<sup>9</sup> was used to give some estimate on the error of the calculations. These yields were taken at 0.1 ms from the calculated concentration profiles.

When air is used as a bath gas, bimolecular reaction of acetyl with O<sub>2</sub> reduces the prompt dissociation yield further and this effect increases as the total pressure, and therefore [O<sub>2</sub>], increases causing the results in air to diverge from those in N<sub>2</sub>. The dissociation yield is almost entirely due to a prompt mechanism, and at 0.1 ms the thermal contribution to dissociation of the CH<sub>3</sub>CO is always less than 5% of the prompt value.

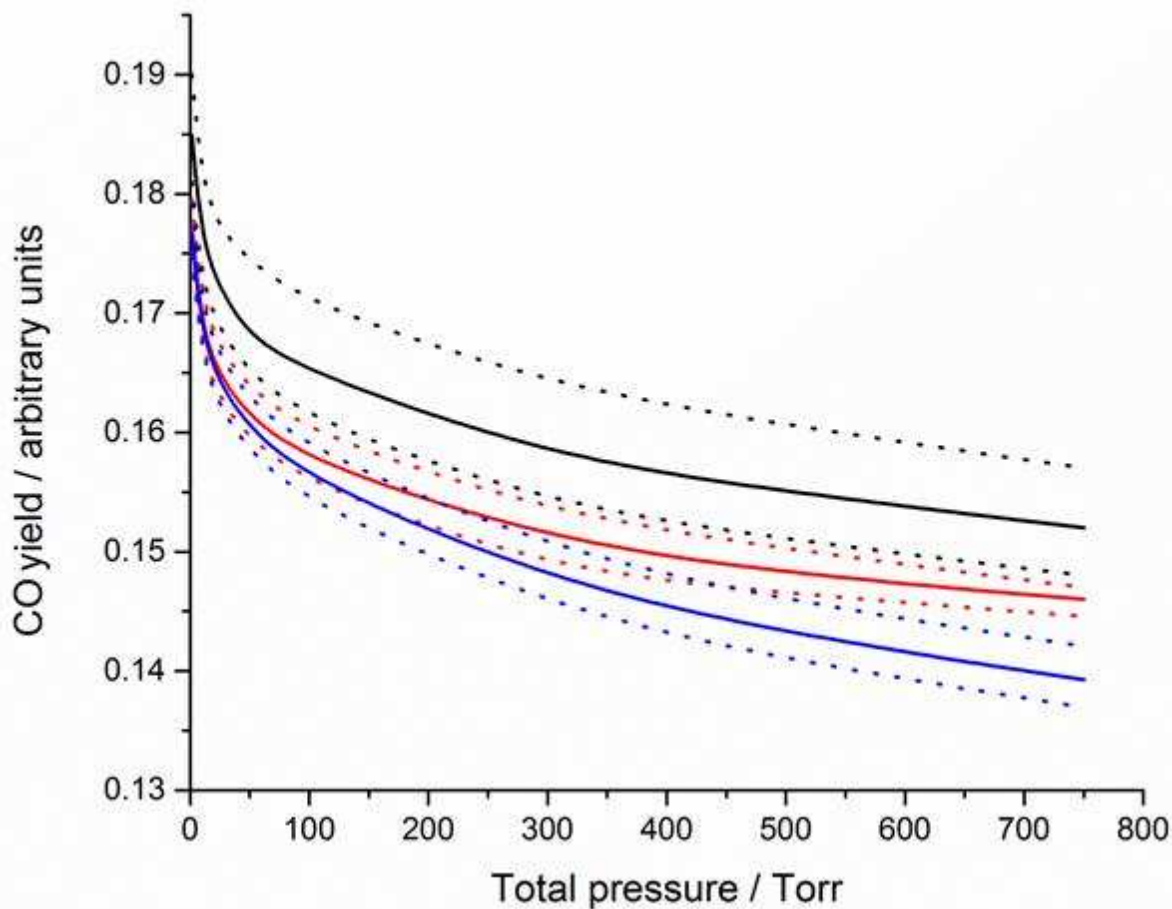


**Figure S9.** Calculated CO yields using MESMER as a function of pressure with three bath gases, He (black), N<sub>2</sub> (red) and air (blue). The dotted lines represent a representative range of  $\langle \Delta E_{\text{down}} \rangle$  values (100-200 cm<sup>-1</sup> for He and 250-350 cm<sup>-1</sup> for N<sub>2</sub> and air).

## 6.0 References

- (1) Baklanov, A. V.; Krasnoperov, L. N. *J. Phys. Chem. A* **2001**, 105, 97.
- (2) Slagle, I. R.; Feng, Q.; Gutman, D. *J. Phys. Chem.* **1984**, 88, 3648.
- (3) Baeza-Romero, M. T.; Blitz, M. A.; Goddard, A.; Seakins, P. W. *Int. J. Chem. Kinet.* **2012**, 44, 532.
- (4) Carr, S. A.; Glowacki, D. R.; Liang, C. H.; Baeza-Romero, M. T.; Blitz, M. A.; Pilling, M. J.; Seakins, P. W. *J. Phys. Chem. A* **2011**, 115, 1069.
- (5) Atkinson, R.; Baulch, D. L.; Cox, R. A.; Crowley, J. N.; Hampson, R. F.; Hynes, R. G.; Jenkin, M. E.; Rossi, M. J.; Troe, J. *Atmos. Chem. Phys.* **2004**, 4, 1461.
- (6) Ianni, J. C. 2002.
- (7) Lee, L. C. *The Journal of Chemical Physics* **1980**, 72, 4334.
- (8) McCabe, D. C.; Smith, I. W. M.; Rajakumar, B.; Ravishankara, A. R. *Chem. Phys. Lett.* **2006**, 421, 111.
- (9) Jasper, A. W.; Miller, J. A. *J. Phys. Chem. A* **2011**, 115, 6438.